Chemical Physics Letters 466 (2008) 247–251

Contents lists available at ScienceDirect

Chemical Physics Letters

journal homepage: www.elsevier.com/locate/cplett

Efficient heteronuclear decoupling by quenching rotary resonance in solid-state NMR

Markus Weingarth [a], Piotr Tekely [a,*], Geoffrey Bodenhausen [a,b]

[a] Département de Chimie, Associé au CNRS, Ecole Normale Supérieure, 24 rue Lhomond, 75231 Paris Cedex 05, France
[b] Institut des Sciences et Ingénierie Chimiques, Ecole Polytechnique Fédérale de Lausanne, Batochime, 1015 Lausanne, Switzerland

ARTICLE INFO

Article history:
Received 27 August 2008
In final form 14 October 2008
Available online 18 October 2008

ABSTRACT

We propose a new scheme for heteronuclear decoupling designed for fast magic-angle spinning (MAS), dubbed phase-inverted supercycled sequence for attenuation of rotary resonance (PISSARRO). Its efficiency compares favourably with CW, TPPM, SPINAL and XiX decoupling methods at medium and high RF amplitudes, particularly under conditions where the efficiency of decoupling is affected by undesired rotary resonance effects.

1. Introduction

Efficient heteronuclear decoupling is one of the most challenging requirements that must be fulfilled to obtain high-resolution NMR spectra of solids. In powders containing directly bonded dilute spins $S = {}^{13}C$ and abundant spins $I = {}^{1}H$, efficient proton decoupling requires a reduction of the heteronuclear dipolar interactions by no less than three orders of magnitude. In polycrystalline or amorphous samples studied by magic-angle spinning (MAS) with slow rotation frequencies ν_{rot} of a few kHz, continuous-wave (CW) irradiation of the abundant I spins with an RF amplitude (also known as nutation or Rabi frequency $\nu_1^I = -\gamma B_1/(2\pi)$) in the range $60 < \nu_1^I < 80$ kHz remains the simplest way to achieve efficient heteronuclear decoupling. At higher spinning speeds, more elaborate schemes have been proposed that use π phase shifted (XiX) [1,2] or two-pulse phase-modulated (TPPM) techniques [3]. The success of these methods has lead to renewed interest in the intricate mechanisms underlying efficient decoupling in rotating solids [4]. Several variants of TPPM [5–8] and more sophisticated decoupling schemes have been developed [9–11].

Recent progress in the design of MAS probes and in superconducting magnet technology, fuelled by the apparently unquenchable demand for enhanced sensitivity and spectral resolution, opens the way to very fast spinning frequencies and to ever-increasing static fields. Higher spinning frequencies lead to a more effective averaging of dipolar interactions. It may be useful to *recouple* dipolar interactions when they give access to structural information. Many recent methodological developments deliberately exploit recoupling to drive the transfer of magnetization from one spin to another. In this Letter, we shall see that recoupling can also occur unwittingly, so that the efficiency of heteronuclear decoupling is compromised. Once identified, it is possible to combat these deleterious effects by suitable phase-modulated schemes.

New recoupling schemes require the design of appropriately tailored RF pulse sequences [12]. One of the simplest methods to recouple dipolar interactions in rotating solids is known as *rotary resonance recoupling* (R^3) [13]. It consists in applying an unmodulated continuous-wave (CW) RF field with an amplitude ν_1 adjusted to fulfil one of the conditions $\nu_1 = n\nu_{rot}$ with $n = 1/2$, 1 and 2 [13,14]. Besides the recovery of the chemical shift anisotropy (CSA) at $n = 1$ and 2, the recoupling of homonuclear interactions can occur at $n = 1/2$ and 1, while heteronuclear interactions are recoupled for $n = 1, 2, 3, \ldots$. Recoupling by rotary resonance has been exploited both for structural studies and to induce a transfer of magnetization [12–19].

However, rotary resonance can also manifest itself through a partial breakdown of the efficiency of heteronuclear dipolar decoupling [20,21], leading to a broadening of the resonances of dilute spins S. To avoid this undesirable broadening, the RF amplitude should be at least 4 times higher than the spinning frequency, i.e., $\nu_1^I > 4\nu_{rot}$ [8,22]. Clearly, with increasing spinning speeds (up to 70 kHz nowadays), it becomes more and more challenging to avoid rotary resonance interferences. Yet, surprisingly, rotary resonance-induced line broadening seems to have been perceived so far as an inevitable collateral damage of the combination of decoupling and spinning. In this work we wish to put this problem into perspective, and describe a method that allows one to quench this type of interference to a large extent.

2. Materials and methods

Polycrystalline powders of L-alanine and calcium formate with natural isotopic abundance, and of uniformly ^{13}C, ^{15}N-labelled L-alanine and L-glycine, were used without further purification.

* Corresponding author. Fax: +33 144 323 344.
E-mail address: Piotr.Tekely@ens.fr (P. Tekely).

0009-2614/$ - see front matter © 2008 Elsevier B.V. All rights reserved.
doi:10.1016/j.cplett.2008.10.041

All experiments were performed on a Bruker spectrometer operating at 9.4 T (Larmor frequency 400.2 MHz for protons), equipped with a 2.5 mm triple resonance MAS probe. In all experiments, cross-polarization (CP) was used to enhance the carbon-13 magnetization, and the MAS frequency was set to $\nu_{rot} = 30$ kHz. The carrier frequency ν_0^I of the decoupling RF field applied to the protons I was systematically placed on-resonance for the protons that are directly attached to the ^{13}C nuclei under observation.

Starting from the original scheme employing simple π phase shifts [1], we developed a new supercycled scheme aimed at attenuating rotary resonance interferences during heteronuclear decoupling. The phase-inverted supercycled sequence for attenuation of rotary resonance (PISSARRO) is composed of pulse pairs $(\tau_p)_x(\tau_p)_{-x}$ and $(\tau_p)_y(\tau_p)_{-y}$ each of which is repeated N times (typically $N = 5$, see below) to form a block, and four blocks are combined as shown in Fig. 1. By constructing such supercycles [9,23], we attenuate rotary resonance interference and minimize higher order heteronuclear terms [9]. The decoupling efficiency of the new scheme has been compared with well-known decoupling methods such as CW, TPPM [3], SPINAL-64 [24] and XiX [1,2] over a wide range of RF amplitudes $40 < \nu_1^I < 140$ kHz. For comparison with the TPPM sequence, the latter's pulse width τ_p and phase angle φ were optimized for each RF amplitude ν_1^I, τ_p being varied in the vicinity of the duration of an ideal π pulse, while the phase angles φ were varied around ±15°. For a given RF-field amplitude ν_1^I, the optimal pulse widths for the SPINAL-64 experiments were found to be close to those for TPPM. For XiX decoupling, the pulse duration τ_p has been optimized around the recommended condition $\tau_p = 2.85 \cdot \tau_{rot}$ [2]. For the PISSARRO sequence, the pulse duration τ_p was optimized for each RF-field amplitude ν_1^I in the interval $0.1 \cdot \tau_{rot} < \tau_p < 2.1 \cdot \tau_{rot}$. The numerical simulations of the CW and PISSARRO decoupling efficiency for a powder average of isolated CH spin systems were performed using the SIMPSON program [25]. Only heteronuclear dipolar couplings (23.3 kHz) were included in the simulations and all isotropic and anisotropic chemical shifts were set to zero. For PISSARRO decoupling the pulse duration was optimized *in silico* for each RF-field amplitude with the same intervals and increments.

To simulate the ^{13}C spectrum of calcium formate with XiX and PISSARRO decoupling at the $n = 2$ rotary resonance condition, we assumed isolated ^{13}C-^{1}H spin pairs with an internuclear distance of 1.09 Å, neglecting chemical shift anisotropies. All simulations used the SIMPSON program [25]. Powder averaging was achieved with 17 γ-angles and 615 α,β-orientations using the Zaremba–Conroy–Wolfsberg (ZCW) scheme [25].

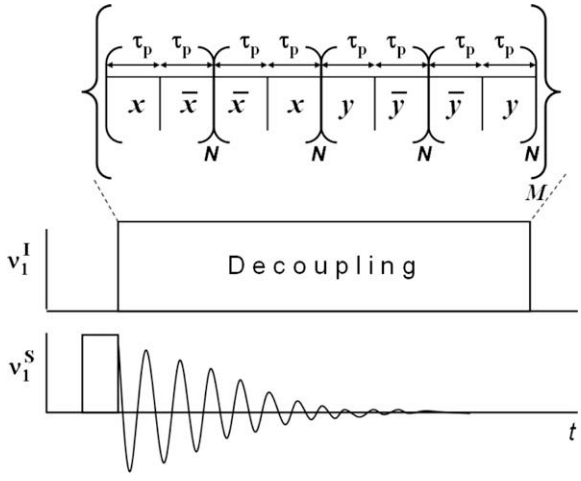

Fig. 1. The PISSARRO scheme for heteronuclear decoupling. The direct excitation of the magnetization of spins S such as ^{13}C can be replaced by cross-polarization from abundant spins I such as protons to the S spins.

3. Results and discussion

To illustrate how rotary resonance recoupling can interfere destructively with decoupling in rapidly spinning powders, Fig. 2 shows plots of ^{13}C signals of L-alanine in natural abundance recorded with CW decoupling as a function of the RF amplitude ν_1^I. Besides a dramatic collapse of all peaks in the vicinity of the rotary resonance conditions $\nu_1^I = n\nu_{rot}$ with $n = 1$ and 2, the plots reveal that the 'dips' around these recoupling conditions extend symmetrically over a wide range of RF amplitudes ν_1^I. Although their breadth can be in part ascribed to the inhomogeneity of the RF-field, since rotary resonance is very sensitive to this parameter [15a], the fact that the dips are the broadest for the rigid CH group must be due to the strength of the heteronuclear dipolar interaction. Note that for the methyl CH_3 and carboxyl COO^- groups, the two dips for $n = 1$ and 2 are much broader than would be expected from the magnitudes of the corresponding heteronuclear couplings. This strongly suggests that homonuclear proton–proton dipolar interactions must also contribute to the breadth of these dips [21] by playing an indirect role in the recoupling conditions at $n = 1$ and 2.

3.1. Quenching of interference of rotary resonance recoupling (R^3) with heteronuclear decoupling

The efficiency of different decoupling sequences for the CH_3, CH_2 and CH groups of uniformly labelled alanine and glycine is

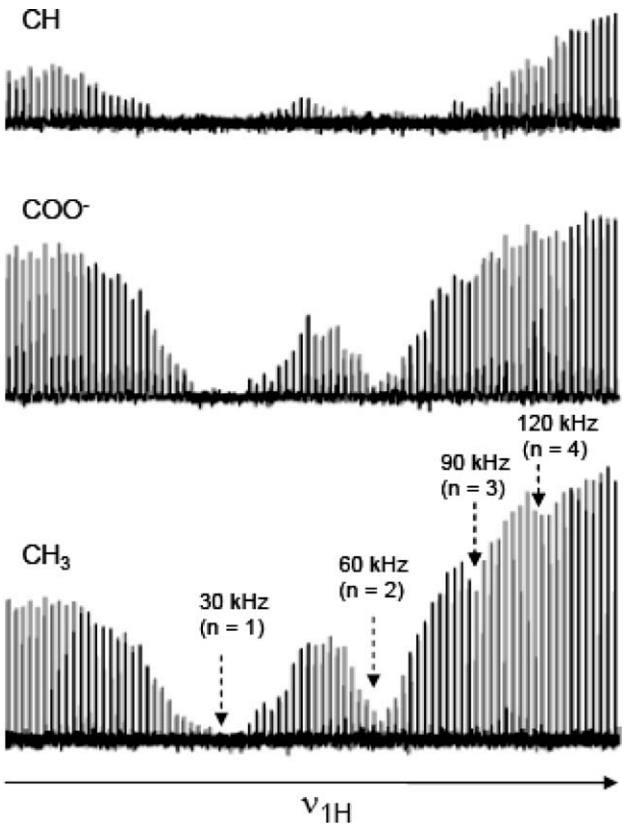

Fig. 2. Efficiency of CW-decoupling in the presence of magic angle spinning (MAS) with a rotation frequency $\nu_{rot} = 30$ kHz. The plots show the ^{13}C resonance signals of the CH_3, COO^- and CH groups in natural abundance L-alanine $NH_3^+CHCH_3COO^-$ as a function of the decoupling radio-frequency (RF) amplitude ν_1^I. Note the broad 'dips' centered at $\nu_1^I = 30$, 60, 90 and 120 kHz, i.e., near the rotary resonance conditions $\nu_1^I = n\nu_{rot}$ with $n = 1$, 2, 3 and 4.

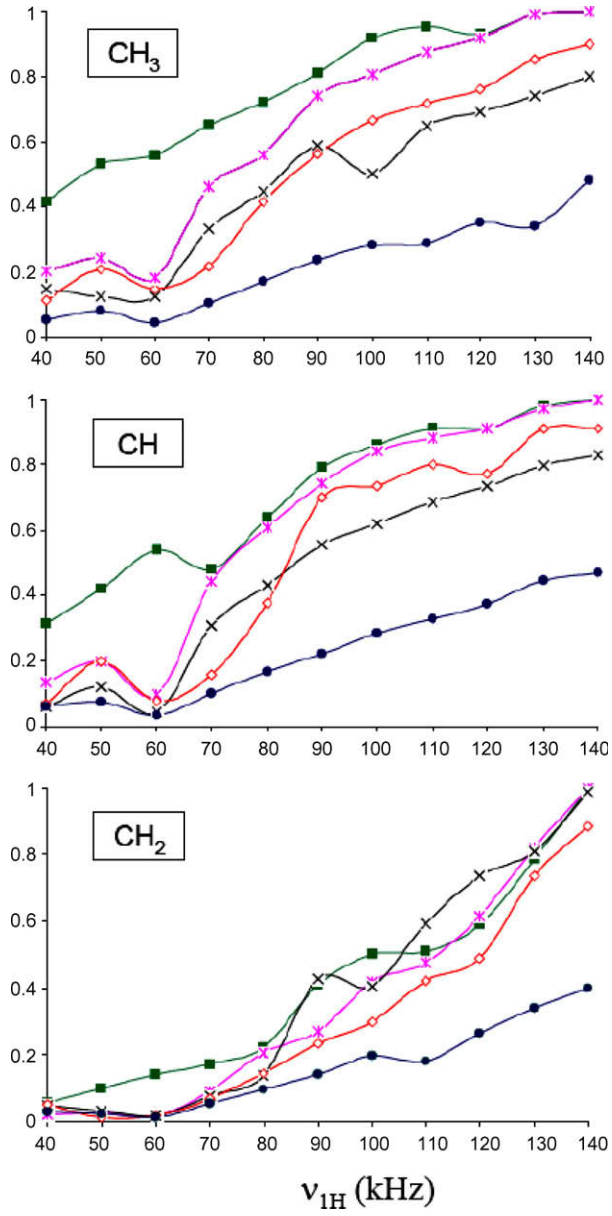

Fig. 3. Comparison of the ^{13}C peak intensity of the CH_3, CH and CH_2 signals in uniformly ^{13}C, ^{15}N-labelled L-alanine and L-glycine, which give a measure of the decoupling efficiency of various decoupling schemes at $\nu_{rot} = 30$ kHz: PISSARRO (green, filled squares), XiX (magenta, stars), TPPM (black, crosses), SPINAL-64 (orange, open squares) and CW (blue, filled circles). (For interpretation of the references to colour in this figure legend, the reader is referred to the web version of this article.)

shown in Fig. 3 over a wide range of RF-amplitudes ν_1^I that include rotary resonance conditions $\nu_1^I = n\nu_{rot}$ with $n = 2$, 3 and 4. For each resonance, the signal intensities were normalized to 1 for the PISSARRO scheme using the highest decoupling amplitude ν_1^I. Besides the obvious improvement in performance of all phase-modulated schemes compared to CW decoupling, the PISSARRO sequence proved to be the most effective in quenching rotary resonance effects in the range $40 < \nu_1^I < 100$ kHz. For CH_3 and CH groups, it turned out to be the most efficient method over the whole range $40 < \nu_1^I < 140$ kHz that could be explored. Indeed, for both CH_3 and carboxyl groups (the latter not shown), the new scheme using $\nu_1^I = 90$ kHz is more efficient than TPPM with $\nu_1^I = 140$ kHz, and for CH_3 and CH groups the new method, again using $\nu_1^I = 90$ kHz, reaches ~80% of the performance of XiX with $\nu_1^I = 140$ kHz. For the CH_2 group of glycine, the PISSARRO scheme was only inferior

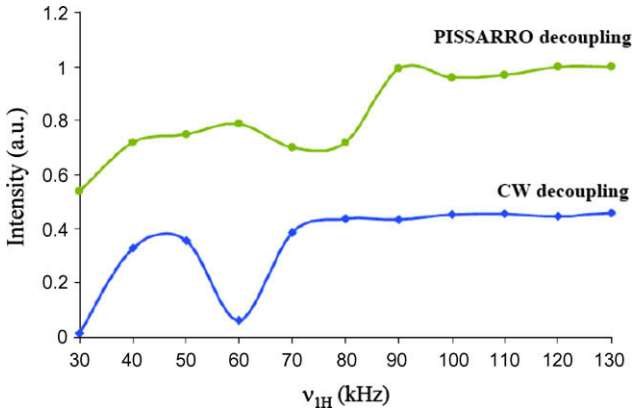

Fig. 4. Numerical simulations of the CW and PISSARRO decoupling efficiency for a powder average of isolated CH spin systems. The spinning frequency was set to 30 kHz. The plots show the line intensities calculated as a function of the RF-field amplitude.

to the TPPM sequence in the range of $110 < \nu_1^I < 130$ kHz, while for $\nu_1^I = 140$ kHz the new method showed the same performance as XiX and TPPM. Obviously, a high decoupling efficiency with moderate RF amplitudes $\nu_1^I < 100$ kHz is particularly attractive for heat-sensitive samples, such as proteins with high water and salt content, where high RF power levels can be harmful. The numerical simulations of CW and PISSARRO decoupling efficiency presented in Fig. 4 using an idealized CH spin system corroborate the experimentally observed quenching of rotary resonance recoupling by the PISSARRO scheme. Extensive numerical simulations will be necessary to probe the influence of homonuclear proton–proton couplings when quenching rotary resonance effects. Indeed, the relevance of such interactions for heteronuclear decoupling in spinning solids has been recognized early on [1], and studied experimentally and theoretically under different conditions [1,9,26–28].

Fig. 5a allows one to appreciate how sensitive various decoupling schemes are to rotary resonance interference at the $n = 2$ condition ($\nu_1^I = 60$ kHz and $\nu_{rot} = 30$ kHz). The relative intensities of the CH_3 signals using PISSARRO, XiX, SPINAL-64, TPPM and CW decoupling are 100%, 33%, 27%, 18% and 8% respectively. The CH_3 linewidths are 83, 126, 163, 250 and 730 Hz for the five methods that have been compared. Note that areas of the signals are not conserved, since the signal amplitudes are partly transferred to modulation sidebands, as discussed below. For the CH resonance, the relative intensities in Fig. 5a are 100%, 18%, 14%, 8% and 7%, and the corresponding linewidths are 135, 218, 285, 760 and 1250 Hz. For the CH_2 resonance, the relative intensities are 100%, 12%, 12%, 13% and 9 %, and the corresponding linewidths 250, 440, 1100, 710 and 1230 Hz. Although at the $n = 2$ rotary resonance condition, the amplitude of the CH_2 signal observed with PISSARRO remains modest compared to high amplitude decoupling (the efficiency of decoupling at $\nu_1^I = 100$ kHz is shown in Fig. 5b), the CH_2 intensity could be increased by a factor of at least 8 compared to other decoupling schemes at this rotary resonance condition. The efficiency of heteronuclear decoupling for the CH resonance signal as a function of the pulse duration τ_p and the RF-field decoupling amplitude ν_1 is shown in two-dimensional contour plot in Fig. 5c. The data reveal that over a wide range $80 < \nu_1^I < 140$ kHz, the optimal τ_p values are near $(0.9 \pm 0.003) \cdot \tau_{rot}$ or $(1.1 \pm 0.003) \cdot \tau_{rot}$ while at lower RF fields including the $n = 2$ condition the recommended τ_p are close to $0.195 \cdot \tau_{rot}$. It should be pointed out that for XiX decoupling, an improved efficiency was observed at $n = 2$ with $\tau_p = 0.85 \cdot \tau_{rot}$, much shorter that the recommended duration $\tau_p = 2.85 \cdot \tau_{rot}$. However, for CH_2, CH and CH_3 groups,

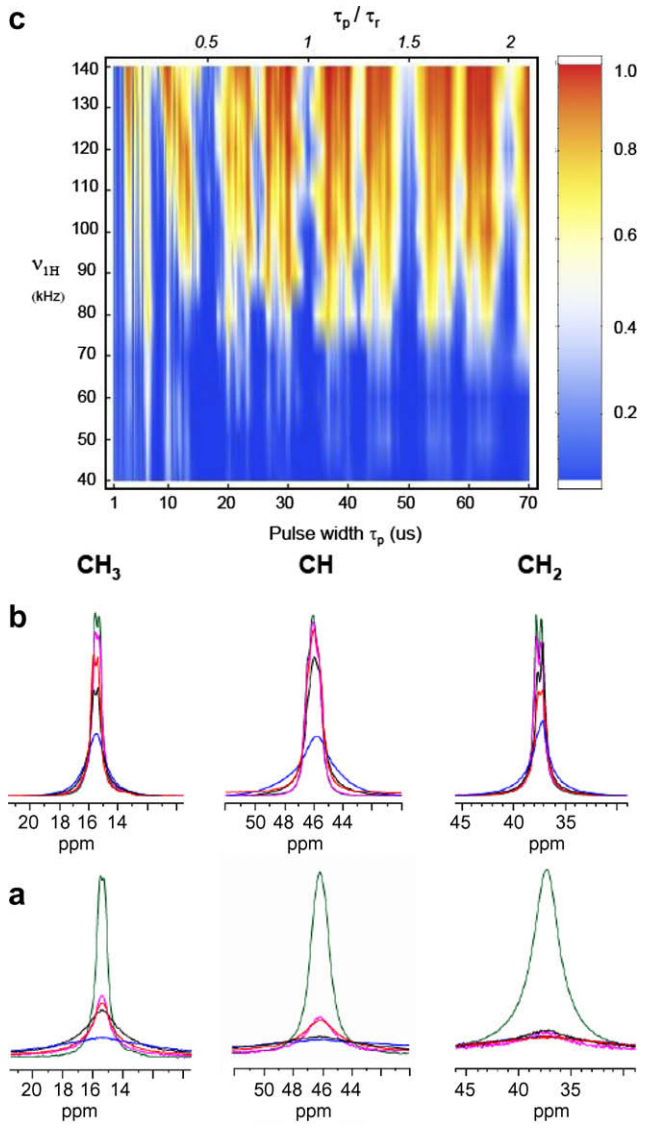

Fig. 5. (a, b) Comparison of the ^{13}C peak intensity of the CH_3, CH and CH_2 signals in uniformly ^{13}C,^{15}N-labelled L-alanine and L-glycine, acquired at $\nu_{rot} = 30$ kHz with (a) $\nu_1^I = 60$ and (b) $\nu_1^I = 100$ kHz, using PISSARRO (green), XiX (magenta), TPPM (black), SPINAL-64 (red) and CW (blue). (c) Two-dimensional contour plot showing the experimental line intensity of the CH group as a function of the pulse length (τ_p) and the RF-field amplitude (ν_{1H}) using the PISSARRO scheme. (For interpretation of the references to colour in this figure legend, the reader is referred to the web version of this article.)

the intensities were around 40%, 45% and 74%, respectively with the new decoupling scheme.

Finally, we note that a simplified, truncated version of the PISSARRO scheme, using only the first half of the decoupling sequence in Fig. 1, without any 90° phase shifts, also exhibits a significantly improved decoupling efficiency at $n = 2$ compared with other pulse sequences. For $70 < \nu_1^I < 80$ kHz, it is actually superior to the complete untruncated PISSARRO scheme, although at $n = 2$ the intensity for CH was only about 70% of that recorded with the complete sequence.

Moreover, the supercycled PISSARRO sequences with odd numbers of pulse pairs $N = 3, 5, 7\ldots$ (usually, $N = 5$) perform significantly better than those with even numbers $N = 2, 4, 6\ldots$

Destructive interference due to rotary resonance recoupling also occurs when very fast spinning frequencies $\nu_{rot} > 30$ kHz are combined with commonly used RF-decoupling schemes. For CH and CH_2 resonances observed with MAS frequencies $\nu_{rot} = 40$ kHz, the effects of rotary resonance interferences can extend beyond $\nu_1^I = 200$ kHz [8] while at $\nu_{rot} = 68$ kHz such effects occur up to $\nu_1^I = 300$ kHz [22]. All previously known decoupling methods therefore entail the use of ever-increasing RF-amplitudes with ever-increasing MAS frequencies. Low-amplitude decoupling with $\nu_1^I << \nu_{rot}$ can be used to alleviate interference effects. Except for CH_2 resonances, this simple approach can compete in efficiency with high amplitude decoupling, provided $\nu_{rot} > 40$ kHz [8,29].

3.2. Quenching of modulation sidebands

Another remarkable advantage of the new PISSARRO scheme is its unique capacity to suppress spurious modulation sidebands, which arise from the interference between the decoupling field and the modulation of dipolar couplings by MAS. Fig. 6a shows spectra recorded at the $n = 2$ rotary resonance condition, with different decoupling schemes optimized for signal intensity. The modulation sidebands show up dramatically for all known techniques except for the new scheme, which offers a remarkably clean spectrum.

Because of the complexity of the evolution of the magnetization under phase-modulated irradiation and MAS close to rotary resonance conditions, the combined effects of homo- and heteronuclear dipolar interactions are difficult to handle analytically. A zeroth order average Hamiltonian theory would be insufficient to shed light on the underlying spin dynamics of rotary resonance quenching. Multimodal Floquet theory could possibly provide some insight, but this is beyond the scope of the present manuscript. To gain a better insight into some basic features of XiX and PISSARRO decoupling, we studied by experiments and simulations the behaviour of calcium formate $Ca(HCOO)_2$ with natural ^{13}C abundance, which contains reasonably isolated ^{13}C–^{1}H spin pairs. Very similar effects could be observed for the (less well isolated) CH group in uniformly ^{13}C enriched L-alanine. As shown in Fig. 6b and c, both the experimental and simulated spectra clearly show the dependence of the modulation sidebands that appear at $\nu_{sb} = K(\pm\nu_{rot} \mp 1/\tau_p)$ on the pulse length τ_p of XiX decoupling. Thus for $\nu_{rot} = 30$ kHz and $\tau_p = 31.5$ μs, i.e., $1/\tau_p = 31.746$ kHz, one obtains sidebands at integer multiples K of 1.746 kHz. These modulation sidebands cannot be removed by optimizing the τ_p values for the best decoupling efficiency. On the other hand, experimental and simulated spectra (Fig. 6d) obtained with the PISSARRO scheme with optimized τ_p values are remarkably free of any spurious sideband signals. Further simulations (not shown) reveal that the magnitudes of the dipolar and CSA interactions, the proton offset and the RF-field amplitude all affect the intensity of the modulation sidebands under XiX decoupling. It is worth noting that the modulation sidebands overlap with their parent signals when τ_p corresponds to a full rotor period ($\nu_{rot} = 1/\tau_p$), thus fulfilling one of the recoupling conditions for phase-alternated decoupling [1,2].

4. Conclusions

We have introduced a novel heteronuclear decoupling scheme for fast MAS that offers improved decoupling efficiency over a wide range of RF-amplitudes ν_1^I. The PISSARRO decoupling sequence using a single adjustable τ_p parameter proved to be more effective than the XiX, TPPM, SPINAL-64 and CW methods in quenching rotary resonance interference effects. The new method yields improved resolution and sensitivity for all solid-state NMR spectra recorded with fast spinning with RF-amplitudes ν_1^I in the vicinity of the $n = 2$ rotary resonance condition. Numerical simulations corroborate the experimental observation that the quenching of rotary resonance effects by the PISSARRO scheme is quite efficient.

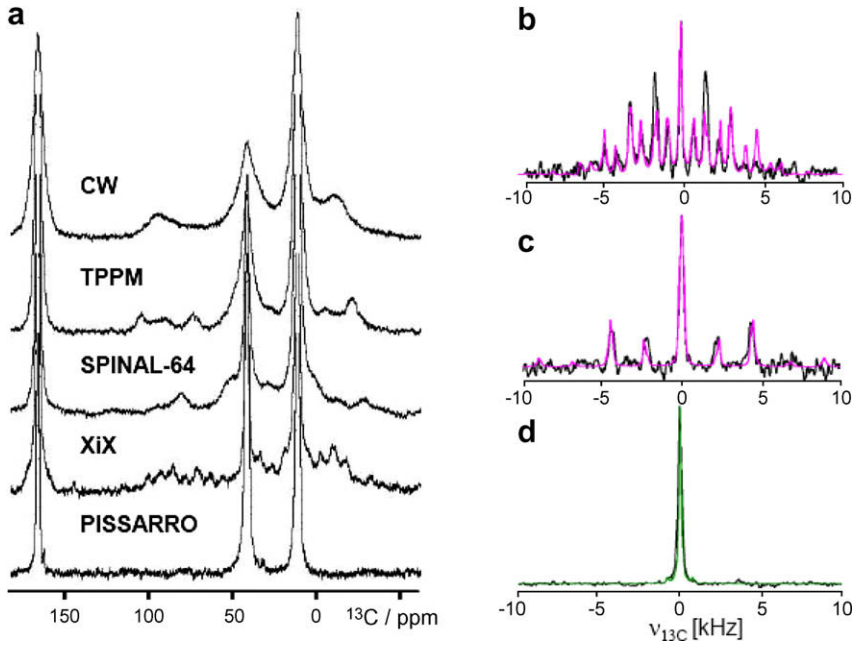

Fig. 6. (a) Comparison of experimental spectra of L-alanine recorded with $\nu_1^I = 60$ kHz and $\nu_{rot} = 30$ kHz ($n = 2$), using the CW, TPPM, SPINAL-64, XiX and PISSARRO decoupling schemes. Note the presence of modulation sidebands that are due to the interference of decoupling and spinning. The sidebands completely disappear with the PISSARRO scheme. (right) Experimental (black) and simulated (magenta and green) spectra of calcium formate obtained with $\nu_1^I = 60$ kHz using the (b, c) XiX and (d) PISSARRO schemes. The simulations were performed for $\nu_{rot} = 30$ kHz with pulse widths (b) $\tau_p = 31.5$ μs, (c) 32.5 μs, and (d) and 6.55 μs. (For interpretation of the references to colour in this figure legend, the reader is referred to the web version of this article.)

For CH_3, COO^- and CH groups, PISSARRO decoupling proved to be the most efficient method over the whole range $40 < \nu_1^I < 140$ kHz that was examined. For the more challenging CH_2 groups, PISSARRO decoupling was less efficient than TPPM in a limited range $110 < \nu_1^I < 130$ kHz. At $\nu_1^I = 140$ kHz the new scheme has the same performance as XiX and TPPM. Since PISARRO decoupling leads to quenching of rotary resonance interference, one can expect an improved efficiency of low amplitude decoupling at high MAS frequencies $\nu_{rot} > 40$ kHz.

Acknowledgements

Financial support of the Agence Nationale de la Recherche (ANR), the Région Ile-de-France (Programme Sesame), the CNRS, the ENS, the EPFL, and the Commission pour la Technologie et l'Innovation (CTI) is gratefully acknowledged.

References

[1] P. Tekely, P. Palmas, D. Canet, J. Magn. Reson. A 107 (1994) 129.
[2] A. Detken, E.H. Hardy, M. Ernst, B.H. Meier, Chem. Phys. Lett. 356 (2002) 298.
[3] A.E. Bennett, C.M. Rienstra, M. Auger, K.V. Lakshli, R.G. Griffin, J. Chem. Phys. 103 (1995) 6951.
[4] P. Hodgkinson, Prog. NMR Spectrosc. 46 (2005) 197 and references therein.
[5] Z. Gan, R.R. Ernst, Solid State NMR 8 (1997) 153.
[6] K. Takegoshi, J. Mizokami, T. Terao, Chem. Phys. Lett. 341 (2001) 540.
[7] R.S. Thakur, N.D. Kurur, P.K. Madhu, Chem. Phys. Lett. 426 (2006) 459.
[8] M. Kotecha, N.P. Wickramasingbe, Y. Ishii, Magn. Reson. Chem. 45 (2007) S221.
[9] M. Eden, M.H. Levitt, J. Chem. Phys. 111 (1999) 1511.
[10] G. De Paëpe, P. Hodgkinson, L. Emsley, Chem. Phys. Lett. 376 (2003) 259.
[11] G. Gerbaud, F. Ziarelli, S. Caldarelli, Chem. Phys. Lett. 377 (2003) 1.
[12] S. Dusold, A. Sebald, Ann. Rep. NMR Spectrosc. 41 (2000) 185.
[13] T.G. Oas, R.G. Griffin, M.H. Levitt, J. Chem. Phys 89 (1988) 692–695.
[14] N.C. Nielsen, H. Bildsoe, H.J. Jakobsen, M.H. Levitt, J. Chem. Phys. 101 (1994) 1805.
[15] (a) Z. Gan, D.M. Grant, R.R. Ernst, Chem. Phys Lett. 254 (1996) 349;
(b) Z. Gan, J. Magn. Reson. 183 (2006) 247.
[16] (a) K. Takegoshi, S. Nakamura, T. Terao, Chem. Phys. Lett. 344 (2001) 631;
(b) K. Takegoshi, S. Nakamura, T. Terao, J. Chem. Phys. 118 (2003) 2325.
[17] Z. Gan, J.P. Amoureux, J. Trébosc, Chem. Phys. Lett. 435 (2007) 163.
[18] L. Odgaard, M. Bak, H.J. Jakobsen, N.C. Nielsen, J. Magn. Reson. 148 (2001) 298.
[19] (a) L. Duma, D. Abergel, P. Tekely, G. Bodenhausen, Chem. Commun. 20 (2008) 2361;
(b) L. Duma, D. Abergel, F. Ferrage, P. Pelupessy, P. Tekely, G. Bodenhausen, ChemPhysChem 9 (2008) 1104.
[20] T. Nakai, C.A. McDowell, Chem. Phys. Lett. 227 (1994) 639.
[21] S.J. Kitchin, K.D.M. Harris, A.E. Aliev, D.C. Apperley, Chem. Phys. Lett. 323 (2000) 490.
[22] M. Ernst, A. Samoson, B.H. Meier, J. Chem. Phys. 123 (2005) 064102-1.
[23] M.H. Levitt, J. Chem. Phys. 128 (2008) 052205-1.
[24] B.M. Fung, A.K. Khitrin, K. Ermolaev, J. Magn. Reson. 142 (2000) 97.
[25] M. Bak, J.T. Rasmussen, N.C. Nielsen, J. Magn. Reson. 147 (2000) 296.
[26] M. Ernst, H. Zimmermann, B.H. Meier, Chem. Phys. Lett. 317 (2000) 581.
[27] G. De Paëpe, B. Elena, L. Emsley, J. Chem. Phys. 121 (2004) 3165.
[28] M. Leskes, R.S. Thakur, P.K. Madhu, N.D. Kurur, S. Vega, J. Chem. Phys. 127 (2007) 024501.
[29] M. Ernst, A. Samoson, B.H. Meier, Chem. Phys. Lett. 348 (2001) 293.